

# A FINITE VOLUME PRESERVING SCHEME ON NONUNIFORM MESHES AND FOR MULTIDIMENSIONAL COALESCENCE\*

L. FORESTIER-COSTE<sup>†</sup> AND S. MANCINI<sup>†</sup>

**Abstract.** In this paper we present a deterministic numerical approximation of the coalescence or Smoluchowski equation. Our numerical scheme conserves the first order momentum and deals with nonuniform grids. The generalization to a multidimensional framework is also described. We validate the scheme considering some classical tests both in one and two dimensions and discuss its behavior when gelation occurs. Our numerical results and code are compared with those already existent in the literature.

**Key words.** finite volume method, nonuniform mesh, coalescence equation

**AMS subject classifications.** 65R20, 82C05

**1. Introduction.** In the last years, the resolution of the coalescence or Smoluchowski equation (see [18]) has been largely studied both from the theoretical and numerical points of view. In fact the successive merging of particles occurs in various physical phenomena spreading from planetary science to aerosols, or polymers (see [14] and references therein). From the numerical point of view, several methods has been proposed for solving the coalescence equation, either starting from the discrete form (see for example [12] and [13]) or considering the continuous form (see [4], [7], [10], [17] and [13] for deterministic methods, or [1], [3], [5], [6] for stochastic ones). More recently, works concerning the numerical resolution of the multidimensional coalescence problem has been proposed (see [17], [11] and references therein).

Our work has been suggested by the study of the growth of gas bubbles in magma, for which a two dimensional framework is needed, since the perfect gas law doesn't holds during the bubbles growth, i.e. bubbles mass and volumes are independent variables. Moreover, recent results in volcanology (see [2] and [8]) highlight that coalescence of gas bubbles growing by decompression and exsolution in the volcano conduit is an important phenomena and may heavily influence the kind of eruption (effusive or explosive). Finally, bubbles coalescence implies that bubbles dimensions may growth of several orders of magnitude and therefore nonuniform meshes are more suitable in order to approximate the domain.

Before entering the details of our study, we first recall the one dimensional continuous and homogeneous in space Smoluchowski equation, we shall refer to as the coalescence equation. Let  $f(x, t)$  denote the distribution function of a set of particles at time  $t$  and with dimension  $x \geq 0$ . Note that, the dimension  $x$  usually represents the mass or the volume of a particle. Then the coalescence equation reads:

$$\partial_t f = \frac{1}{2} \int_0^x H(x', x - x') f(x') f(x - x') dx' - f(x) \int_0^\infty H(x, x') f(x') dx' \quad (1.1)$$

where the coalescence kernel  $H(x, x')$  represents the rate of merging particles of dimension  $x$  and  $x'$ ; it is assumed to be positive,  $H(x, x') > 0$ , and symmetric,  $H(x, x') = H(x', x)$ . The first term on the right-hand side of equation (1.1), represents the gain term and it accounts for those particles of dimension  $x'$  merging with

\*This work was partially founded by the ERC-starting grant DEMONS (n. 202844) under the European FP7.

<sup>†</sup>Fédération Denis Poisson (FR 2964), MAPMO (UMR 6628), BP. 6759, Université d'Orléans, F-45067 Orléans, France. (simona.mancini@univ-orleans.fr)

particles of dimension  $x - x'$  and giving particles of dimension  $x$ . In other words, when two particles merge their dimensions just sum up, so that coalescence process conserves the total dimension of the particles involved with. The second term on the left-hand side of equation (1.1) is the loss term and accounts for those particles of dimension  $x$  which disappear by coalescing with particles of dimension  $x'$ . The more general formulation for the coalescence kernel reads, see for example [7]:

$$H(x, x') = x^\mu (x')^\nu + x^\nu (x')^\mu, \quad 0 \leq \mu \leq \nu \leq 1. \quad (1.2)$$

As we are interested here on the numerical validation of our scheme, we restrict our study to the following coalescence kernels which are interesting for mathematical aspects, since the coalescence equation (1.1) admits explicit solutions for them, but which aren't physically relevant. Choosing in (1.2),  $\mu = \nu = 0$  or  $\mu = \nu = 1$ , we respectively obtain, up to a factor 2, the constant kernel  $H(x, x') = 1$  and the multiplicative one  $H(x, x') = xx'$ . We shall also consider the kernel  $H(x, x') = x + x'$  obtained by choosing in (1.2)  $\mu = 1$  and  $\nu = 0$ , or vice versa. Finally we note that all these coalescence kernels are independent on time, but it is easy to generalize our numerical scheme to time dependent kernels.

Let us now denote by  $M_p(t)$ , the  $p^{\text{th}}$  order moments associated to the distribution function  $f(t, x)$ :

$$\mathcal{M}_p(t) = \int_0^\infty x^p f(x, t) dx. \quad (1.3)$$

For instance, when  $p = 0, 1$ , the zero and the first order moments,  $\mathcal{M}_0$  and  $\mathcal{M}_1$ , respectively represent the density number of particles and their total dimension (total mass or volume). It is well known that, when considering the constant coalescence kernel  $H(x, x') = 1$  or the additive one  $H(x, x') = x + x'$ , the first order moment conserved in time. Whereas, the zero and second order moments are respectively decreasing and increasing in time. On the other hand, when considering the multiplicative coalescence kernel,  $H(x, x') = xx'$ , the gelation phenomena occurs, as was proved in [15]. This means that, due to the fast increment of the coalescence kernel, a runaway growth leads to the formation of particles with infinite dimension in finite time. Briefly, some matter escape from the system of particles, so that the first order moment  $\mathcal{M}_1$  is not conserved, but decreases in time, see for example [7].

We finally recall that equation (1.1) can be written in the following conservative form, see for example [19] and [7]:

$$x \partial_t f = -\partial_x \int_0^x \int_{x-u}^\infty u H(u, v) f(v) f(u) dv du. \quad (1.4)$$

Many numerical schemes dealing with the discretisation of equation (1.1) or (1.4) have been proposed in recent years, and it would be not possible to give an exhaustive list. In this paper, we will compare and validate our numerical scheme with respect to [7] and [17] concerning the one dimensional case, and with respect to [17] concerning the multidimensional case. In particular, in [7] the numerical scheme is based on a finite volume discretization of (1.4), which is robust for nonuniform meshes, the conservation of the first order moment being implicitly given by the conservative form (1.4). The multidimensional numerical scheme described in [17] is the generalization of the one proposed in [12] and is also based on a finite volume method. The conservation of the first order moment and the handling of nonuniform meshes are thus ensured

for discrete particles, but their solutions in the two dimensional framework show singularities.

In this paper, we propose a numerical scheme based on a finite volume approach for equation (1.1), which deals with nonuniform meshes and the overlaps of the created particles with the defined mesh, and which conserves the discrete first order moment. Moreover, our scheme is second order accurate and thus consistent. Finally, the generalisation to the multidimensional framework is straight forward. The discretisation itself, will be detailed in the one dimensional framework, but, as said, the numerical validation will be done both for the one dimensional and the two dimensional cases.

This paper is organised as follows. In section 2 we detail the numerical approximation in the one dimensional framework. Section 3 is devoted to the multidimensional generalization of the given numerical scheme. Numerical results and the validation of the code are presented and discussed both for the one and two dimensional problems in section 4. Finally, section 5 resumes our results and presents research axes for future works.

**2. One dimensional scheme.** Let us first write the one dimensional numerical scheme we will apply in our simulations. How to obtain it as well as how to handle the overlap and the first order moment conservation will be described in sections 2.1 and 2.2.

We choose to discretize the coalescence equation (1.1) applying a finite volume approximation, since this method seems to be the more natural when having to deal with nonuniform meshes. Let us split  $\mathbb{R}^+$  in the cells  $i = [x_{i-1/2}, x_{i+1/2}]$ , for  $i \in \mathbb{N}$ , with the usual definition  $x_{-1/2} = 0$ , see for example [7], and let us define the grid points by:

$$x_i = \frac{x_{i-1/2} + x_{i+1/2}}{2},$$

and the mesh step by:

$$\Delta x_i = x_{i+1/2} - x_{i-1/2}.$$

We shall denote in the sequel the merging of two cells  $j$  and  $k$  giving a cell  $i$  by  $i = (j+k)$ , so that the bounds of the created cell are given by  $x_{i-1/2} = x_{j-1/2} + x_{k-1/2}$  and  $x_{i+1/2} = x_{j+1/2} + x_{k+1/2}$ .

Moreover, for  $n \in \mathbb{N}$ , let us consider the discrete time  $t^{n+1} = t^n + \Delta t^n$ . Hence, the discrete distribution function  $f_i^n$  defined at the iteration  $n$  on the cell  $i$  is given by  $f_i^n = f(x_i, t^n)$  and the discrete coalescence kernel  $H_{i,j}$  by  $H_{i,j} = H(x_i, x_j)$ , for  $i$  and  $j \in \mathbb{N}$ . With this notations, our finite volume numerical approximation will read:

$$f_i^{n+1} = f_i^n + \Delta t^n \left( \frac{1}{2} \sum_{(j,k) \in S^i} \tilde{H}_{j,k} f_j^n f_k^n \lambda_{j,k}^i \frac{\Delta x_j \Delta x_k}{\Delta x_i} - \sum_{j=0}^{\infty} H_{i,j} f_i^n f_j^n \Delta x_j \right) \quad (2.1)$$

where  $\tilde{H}_{j,k}$  is a modified kernel ensuring the first order moment conservation. Moreover, defining the set  $S^i$  by:

$$S^i = \{(j, k) \in \mathbb{N} \times \mathbb{N} : (j+k) \cap i \neq \emptyset\},$$

the term  $\sum_{(j,k) \in S^i}$  represents, for a fixed cell  $i$ , the sum over all possible cells  $k$  and  $j$  such that the intersection of their sum with the cell  $i$  isn't empty. We finally remark

that if, for example, given a constant  $h$ , the mesh is of the form  $x_i = i^3 h$  (as it is the case in our volcanology problem), then from the Fermat theorem it follows that, given a cell  $j$  and a cell  $k$ , it doesn't exist a cell  $i$  such that we exactly have  $i = (j + k)$ , see [21]. Hence the cell  $i$  must overlap one or more cells, and the proportionality parameter  $\lambda_{j,k}^i$ , defined by (2.5), accounts for this overlap.

**2.1. Cells overlap.** In this section we explain how we handle the cells overlap, that is how we compute the term  $\sum_{(j,k) \in S^i}$ . Let us first write the finite volume discretization for (1.1). Integrating it over a cell  $i$ , we have:

$$\partial_t \int_{x_{i-1/2}}^{x_{i+1/2}} f dx = \frac{1}{2} \int_{x_{i-1/2}}^{x_{i+1/2}} \int_0^x H(x-x', x') f(x-x') f(x') dx' dx - \int_{x_{i-1/2}}^{x_{i+1/2}} \int_0^\infty H(x, x') f(x) f(x') dx' dx. \quad (2.2)$$

Then applying a midpoint quadrature formula, the term on the left-hand side of (2.2) easily reads as:

$$\partial_t f_i(t) \Delta x_i, \quad (2.3)$$

and the last term on the right-hand side of (2.2), that is the loss term, becomes:

$$\sum_{j=0}^{\infty} H_{i,j} f_i f_j \Delta x_i \Delta x_j. \quad (2.4)$$

Concerning the gain term, that is the first term on the right hand side in (2.2), some work is needed in order to handle the  $x - x'$  variable.

Before dealing with the discretization of the gain term in (2.2), let us introduce and define some elements we will need. When considering nonuniform grids, the sum of two cells, say  $j$  and  $k$ , may give a cell, say  $i$ , overlapping various cells and which extrema do not coincide with the extrema of the cell  $j + k$ . In figure 2.1 we show the three basic configuration of overlaps, but we may have any combination of them.

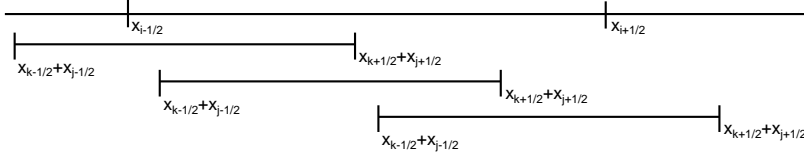


FIG. 2.1. Three basic configurations for overlaps

Let us introduce  $\overline{m_{j,k}^i}$  and  $\underline{m_{j,k}^i}$  respectively denoting the maximum and minimum bounds of the intersection of the cell  $j + k$  with a given cell  $i$ :

$$\overline{m_{j,k}^i} = \max(x_{i-1/2}, x_{j-1/2} + x_{k-1/2})$$

$$\underline{m_{j,k}^i} = \min(x_{i+1/2}, x_{j+1/2} + x_{k+1/2}),$$

and let us define the proportionality factor  $\lambda_{j,k}^i$ , for a given cell  $i$ , as follows:

$$\lambda_{j,k}^i = \left( \frac{\overline{m_{j,k}^i} - \underline{m_{j,k}^i}}{\Delta x_j + \Delta x_k} \right)_+. \quad (2.5)$$

We note that the proportionality parameter is such that:  $0 \leq \lambda_{j,k}^i \leq 1$ , the equality sign holding either when the intersection is empty ( $\lambda_{j,k}^i = 0$ ) or when the sum of the cells  $j + k$  is entirely contained in the cell  $i$  ( $\lambda_{j,k}^i = 1$ ). We also remark that it is symmetric:  $\lambda_{j,k}^i = \lambda_{k,j}^i$ , and that fixing  $j$  and  $k$ , and denoting by  $R_{j,k}$ , the set of all cells  $i$  such that the intersection of  $i$  with  $j + k$  isn't empty, that is:

$$R_{j,k} = \{i \in \mathbb{N} : i \cap (j + k) \neq \emptyset\},$$

then:

$$\sum_{i \in R_{j,k}} \lambda_{j,k}^i = 1.$$

PROPOSITION 2.1. *If we consider the uniform mesh  $x_{i-1/2} = i\Delta x$ , for  $i \in \mathbb{N}$ , then:*

$$\lambda_{j,k}^i = \begin{cases} 1/2 & \text{if } i = \{j + k, j + k + 1\} \\ 0 & \text{otherwise.} \end{cases}$$

**Proof:** Let us consider the sum of the two cells indexed by  $j$  and  $k$  and giving a cell  $i$ , then the new cell  $i$  will have bounds:

$$x_{i-1/2} = x_{j-1/2} + x_{k-1/2} = (j + k)\Delta x,$$

$$x_{i+1/2} = x_{j+1/2} + x_{k+1/2} = (j + k + 2)\Delta x,$$

Hence, the dimension of the new cell  $i$  is  $2\Delta x$ , and since its centre  $x_i$  is given by:

$$x_i = (j + k + 1)\Delta x,$$

it exists  $s \in \mathbb{N}$  such that, by definition of the uniform mesh,  $x_{s-1/2} = x_i$ . In other words, the centre of the new cell  $i$  fall on the lower border of the mesh indexed by  $s = j + k + 1$ . Therefore it seems reasonable that the created cell  $i$  with centre in  $s$  and dimension  $2\Delta x$  just covers the cells  $s$  and  $s - 1$ . Finally, computing  $\lambda_{j,k}^s$  and  $\lambda_{j,k}^{s-1}$  by means of (2.5), we get:  $\lambda_{j,k}^s = \lambda_{j,k}^{s-1} = 1/2$ . ■

We now come back to the discretization of the gain term in (2.2). We omit for simplicity the time dependence of the distribution function  $f(x, t)$ . Inverting the order of integration, applying the change of variable  $z = x - x'$ , inverting again the order of integration and replacing  $z$  by  $x$ , the gain term in (2.2) splits in the sum of two integrals defined respectively on the intervals  $[0, x_{i+1/2}] \times [0, x_{i+1/2} - x']$  and  $[0, x_{i-1/2}] \times [0, x_{i-1/2} - x']$ :

$$\begin{aligned} \int_{x_{i-1/2}}^{x_{i+1/2}} \int_0^x H(x - x', x') f(x - x') f(x') dx' dx = & \quad (2.6) \\ & \int_0^{x_{i+1/2}} \int_0^{x_{i+1/2} - x'} H(x', x) f(x') f(x) dx dx' - \\ & \int_0^{x_{i-1/2}} \int_0^{x_{i-1/2} - x'} H(x', x) f(x') f(x) dx dx'. \end{aligned}$$

The two integrals on the right-hand side of (2.6) are approximated by means of the same technique. We thus detail only the first one. It can be splitted in the sum of the integrals defined on each cell  $j$ , with  $j \leq i$ . That is:

$$\sum_{j=0}^i \int_{x_{j-1/2}}^{x_{j+1/2}} \int_0^{x_{i+1/2}-x'} H(x', x) f(x') f(x) dx dx'. \quad (2.7)$$

In order to take into account the overlap, let us define the indexes  $I_i(j)$  and  $J_i(j)$  such that they are the largest integers verifying:

$$x_{I_i(j)+1/2} + x_{j+1/2} < x_{i+1/2} \quad \text{and} \quad x_{J_i(j)-1/2} + x_{j-1/2} < x_{i+1/2},$$

where the first condition says that the integer  $I_i(j)$  is such that the upper bound of the created cell  $I_i(j) + j$  must be smaller than the one of the cell  $i$ ; and the second condition says that the integer  $J_i(j)$  is such that the lower bound of the created cell  $J_i(j) + j$  must be smaller than the upper bound of the cell  $i$ . Moreover, note that for all  $j \geq i$  the indexes  $I_i(j)$  and  $J_i(j)$  doesn't exists.

The overlap then appears in between  $I_i(j)$  and  $J_i(j)$ . In other words, in (2.7) the second integral can be splitted in the sum of all the integrals defined on the cells such that, when summed with the cell  $j$ , they have the upper bound smaller than  $I_i(j)$  and those for which the summed lower bound is bigger than  $I_i(j)$  and smaller than  $J_i(j)$ . This gives:

$$\sum_{j=0}^i \int_{x_{j-1/2}}^{x_{j+1/2}} \left( \sum_{k=0}^{I_i(j)} \int_{x_{k-1/2}}^{x_{k+1/2}} H(x', x) f(x') f(x) dx + \sum_{k=I_i(j)+1}^{J_i(j)} \int_{x_{k-1/2}}^{x_{k+1/2}} H(x', x) f(x') f(x) \lambda_{j,k}^i dx \right) dx'. \quad (2.8)$$

Note that the proportionality coefficient  $\lambda_{j,k}^i$  appears only in the second sum, since in the first one it is equal to 1, being the summed cells entirely contained in the cell  $i$ . Analogously, the second integral on the right-hand side of (2.6) writes:

$$\sum_{j=0}^{i-1} \int_{x_{j-1/2}}^{x_{j+1/2}} \left( \sum_{k=0}^{I_{i-1}(j)} \int_{x_{k-1/2}}^{x_{k+1/2}} H(x', x) f(x') f(x) dx + \sum_{k=I_{i-1}(j)+1}^{J_{i-1}(j)} \int_{x_{k-1/2}}^{x_{k+1/2}} H(x', x) f(x') f(x) \lambda_{j,k}^{i-1} dx \right) dx'. \quad (2.9)$$

We can now apply a quadrature formula to (2.8) and (2.9) and arrange their sum as follows:

$$\begin{aligned} \sum_{j=0}^i \left( \sum_{k=I_{i-1}(j)+1}^{I_i(j)} H_{j,k} f_j f_k \Delta x_j \Delta x_k + \sum_{k=I_i(j)+1}^{J_i(j)} H_{j,k} f_j f_k \lambda_{j,k}^i \Delta x_j \Delta x_k - \sum_{k=I_{i-1}(j)+1}^{J_{i-1}(j)} H_{j,k} f_j f_k \lambda_{j,k}^{i-1} \Delta x_j \Delta x_k \right) + \sum_{k=0}^{I_{i-1}(i)} H_{i,k} f_i f_k \Delta x_i \Delta x_k + \\ \sum_{k=I_{i-1}(i)+1}^{J_{i-1}(i)} H_{i,k} f_i f_k \lambda_{i,k}^{i-1} \Delta x_i \Delta x_k. \end{aligned} \quad (2.10)$$

Concerning the last two terms in (2.10), since  $I_{i-1}(i)$  and  $J_{i-1}(i)$  do not exist, these sums are null. Therefore, the numerical approximation of the gain term in (2.2) reads:

$$\sum_{j=0}^i \left( \sum_{k=I_{i-1}(j)+1}^{I_i(j)} H_{j,k} f_j f_k \Delta x_j \Delta x_k + \sum_{k=I_i(j)+1}^{J_i(j)} H_{j,k} f_j f_k \lambda_{j,k}^i \Delta x_j \Delta x_k - \sum_{k=I_{i-1}(j)+1}^{J_{i-1}(j)} H_{j,k} f_j f_k \lambda_{j,k}^{i-1} \Delta x_j \Delta x_k \right), \quad (2.11)$$

which we write in a compact form as:

$$\sum_{(j+k) \in S^i} H_{j,k} f_j f_k \lambda_{j,k}^i \Delta x_j \Delta x_k. \quad (2.12)$$

We now detail the three sums appearing in (2.11). The portion of cells over which each sum is computed is represented in figures 2.2 to 2.4 by the dashed lines:

1. The first sum is the integral over the cells  $j$  and  $k$  such that:

$$(j, k) \in S^i \quad \text{and} \quad x_{j+1/2} + x_{k+1/2} < x_{i+1/2}$$

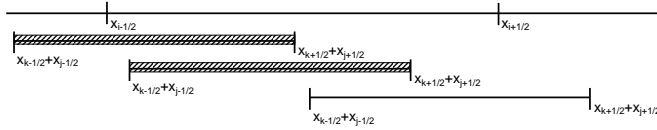


FIG. 2.2. *first sum representation*

2. The second sum is the integral on the cells  $j$  and  $k$  such that:

$$(j, k) \in S^i \quad \text{and} \quad x_{j+1/2} + x_{k+1/2} > x_{i+1/2}$$

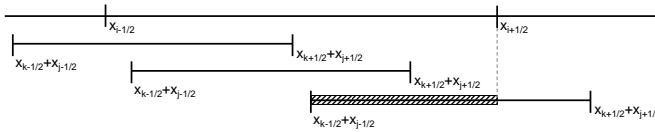


FIG. 2.3. *second sum representation*

3. The third sum is the integral on the cells  $j$  and  $k$  such that:

$$(j, k) \in S^{i-1} \quad \text{and} \quad x_{j+1/2} + x_{k+1/2} > x_{(i-1)+1/2} = x_{i-1/2}$$

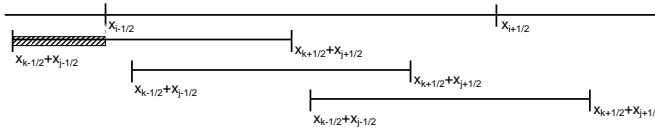


FIG. 2.4. *third sum representation*

Finally, collecting together (2.3), (2.4) and (2.12), the finite volume discretization of equation (1.1) becomes:

$$f_i^{n+1} = f_i^n + \Delta t^n \left( \frac{1}{2} \sum_{(j,k) \in S^i} H_{j,k} f_j^n f_k^n \lambda_{j,k}^i \frac{\Delta x_j \Delta x_k}{\Delta x_i} - \sum_{j=0}^{\infty} H_{i,j} f_i^n f_j^n \Delta x_j \right) \quad (2.13)$$

While (2.13) is constructed in order to take care of the overlaps in the nonuniform mesh framework, the conservation of the first order moment at a numerical level is not ensured, and we shall deal with it in the next section.

**2.2. First order moment conservation.** We want to give a numerical approximation of the coalescence equation (1.1) conserving the discrete first order moment, since we know that the first order moment is conserved at the continuous level. In order to ensure this conservation, we choose to modify the discrete coalescence kernel  $H_{j,k}$  in the gain term by defining a kernel  $\tilde{H}_{j,k}$  in such a way that the previous property holds true for every discrete time  $t^n$ .

Let us first define the discrete moment of order  $p$ . Considering the definition (1.3) at the continuum level, the discrete momentum of order  $p$  at time  $t^n$ ,  $M_p^n = M_p(t^n)$ , is given by:

$$M_p^n = \sum_{i=0}^{\infty} x_i^p f_i^n \Delta x_i. \quad (2.14)$$

Hence, the first order moment conservation reads, for  $p = 1$  and  $n \in \mathbb{N}$ :

$$\sum_{i=0}^{\infty} f_i^{n+1} x_i \Delta x_i = \sum_{i=0}^{\infty} f_i^n x_i \Delta x_i.$$

Therefore, replacing in (2.13)  $H_{j,k}$  by  $\tilde{H}_{j,k}$ , multiplying it by  $x_i$  and summing over all  $i$  we must have:

$$\frac{1}{2} \sum_{i=0}^{\infty} \sum_{(j,k) \in S^i} \tilde{H}_{j,k} f_j^n f_k^n \lambda_{j,k}^i x_i \Delta x_j \Delta x_k = \sum_{i=0}^{\infty} \sum_{j=0}^{\infty} H_{i,j} f_i^n f_j^n x_i \Delta x_j \Delta x_i \quad (2.15)$$

**PROPOSITION 2.2.** *The discrete first order moment (2.14) is conserved if and only if the modified kernel  $\tilde{H}_{j,k}$  is defined by:*

$$\tilde{H}_{j,k} = H_{j,k} \frac{x_j + x_k}{\sum_{i \in R_{j,k}} x_i \lambda_{j,k}^i}. \quad (2.16)$$

**Proof:** Let us first remark that equation (2.15) can be written using tensors algebra as follows:

$$\tilde{\mathbb{H}} : \mathbb{F} = \mathbb{H} : \mathbb{F}, \quad (2.17)$$

where  $\mathbb{F}$ ,  $\mathbb{H}$  and  $\tilde{\mathbb{H}}$  respectively are the following tensors:

$$\mathbb{F} = \sum_{i,j} \mathbb{F}_{ij} \mathbb{E}_{ij}, \quad \mathbb{H} = \sum_{i,j} \mathbb{H}_{ij} \mathbb{E}_{ij}, \quad \tilde{\mathbb{H}} = \sum_{j,k} \tilde{\mathbb{H}}_{jk} \mathbb{E}_{jk}$$

with  $\mathbb{E}_{ij} = \delta_{ij}$ , the base of the matrix set  $\mathbb{M}(\mathbb{R})$ , and with  $\mathbb{F}_{ij} = f_i^n f_j^n$ ,  $\mathbb{H}_{ij} = H_{i,j} x_i \Delta x_i \Delta x_j$  and

$$\tilde{\mathbb{H}}_{jk} = \frac{1}{2} \tilde{H}_{j,k} \left( \sum_{i=0}^{\infty} x_i \lambda_{jk}^i \mathbb{1}_{i \in R_{j,k}} \right) \Delta x_j \Delta x_k,$$

the respective coefficients matrix. Therefore, solving (2.17) is equivalent to determine the coefficients  $\tilde{H}_{j,k}$ . Note that (2.17) is linear in  $\mathbb{F}$ , so that we will verify it only for the basis elements  $\mathbb{E}_{ij}$ .

Hence, let us assume that  $\mathbb{F}_{ij} = \mathbb{E}_{ij}$  that is  $f_i^n = f_j^n = 1$  and  $f_k^n = 0$  for all  $k \neq i, j$ . Then the right-hand side in (2.17), or equivalently in (2.15), gives:

$$(x_i + x_j) H_{i,j} f_i^n f_j^n \Delta x_i \Delta x_j.$$

Concerning the left-hand side of (2.17), or equivalently of (2.15), since the first sum is done for all  $i$ , we surely find one (or more) index  $s$  such that  $(j, i) \in S^s$ , then choosing  $j = j$  and  $k = i$  in the left-hand side of (2.15), we have:

$$\sum_{s \in R_{i,j}} \tilde{H}_{i,j} f_i^n f_j^n \lambda_{i,j}^s x_s \Delta x_i \Delta x_j.$$

Hence, recalling the first moment conservation given by (2.15), the two above quantities must be equal:

$$\sum_{s \in R_{i,j}} \tilde{H}_{i,j} f_i^n f_j^n \lambda_{i,j}^s x_s \Delta x_i \Delta x_j = (x_i + x_j) H_{i,j} f_i^n f_j^n \Delta x_i \Delta x_j.$$

Finally, it is easily seen that the above relation holds if and only if the coefficients  $\tilde{H}_{i,j}$  are defined by (2.16). ■

**PROPOSITION 2.3.** *In the uniform grid framework the modified kernel  $\tilde{H}_{j,k}$  reduces to  $H_{j,k}$ .*

**Proof:** As proved in Proposition 2.1, the only cells  $i$  for which the  $\lambda_{j,k}^i$  in (2.16) are not zero are  $i = j + k + 1$  and  $i = j + k$ . Hence from relation (2.16), recalling the definition of  $x_i$  and of  $\lambda_{j,k}^i$ , and simplifying, we get:

$$\tilde{H}_{j,k} = H_{j,k} \frac{x_j + x_k}{(x_{j+k+1} + x_{j+k})/2} = H_{j,k} \frac{2(j+k+1)}{2j+2k+2} = H_{j,k},$$

concluding the proof. ■

We finally give the CFL condition on the time step needed to ensure the positivity of the numerical solution  $f_i^n$ . Denoting respectively by  $G_i^n$  and  $L_i^n$  the gain and loss integrals in (2.1), we have the following:

**PROPOSITION 2.4.** *If the initial condition  $f_i^0$  is non-negative, then under the following stability condition on the time step:*

$$\Delta t^n < \min_i \left( \left| \frac{f_i^n}{G_i^n - L_i^n} \right| \right). \quad (2.18)$$

*the solution  $f_i^n$  remains positive for each time  $t^n$ .*

We finally remark that our scheme is consistent . In fact, considering a constant distribution function  $f(x, t)$ , then the loss term (2.4) corresponds to the rectangle approximation of  $\int H(x, x') dx'$ . Concerning the gain term, consistency may be proved repeating the same procedure applied to deduce (2.11), but with  $f(x, t)$  constant. Nevertheless, from the numerical results, we deduce that our scheme is second order accurate and thus it is consistent.

**3. Multidimensional discretization.** Before dealing with the validation of the numerical scheme (2.1), we give in this section the generalization to the multi-dimensional case. In fact, as explained in the introduction, our study is suggested by an application in volcanology concerning two dimensional distribution functions  $f(t, x, y)$ . In the sequel we will detail the multidimensional generalization of our scheme, although the numerical simulations are performed in the two dimensional framework.

For  $d > 1$ , let  $\vec{x} \in \mathbb{R}_+^d$  and  $t > 0$ , let also  $f(\vec{x}, t)$  denote the distribution function of particles of dimensions  $\vec{x} = \{x_r\}$ ,  $r = 1 \dots d$ , at time  $t$ . Then the coalescence equation reads:

$$\partial_t f = \frac{1}{2} \int_0^{\vec{x}} H(\vec{x}', \vec{x} - \vec{x}') f(\vec{x}') f(\vec{x} - \vec{x}') d\vec{x}' - \int_0^{\infty} H(\vec{x}, \vec{x}') f(\vec{x}) f(\vec{x}') d\vec{x}', \quad (3.1)$$

where

$$d\vec{x}' = \prod_{r=1}^d dx'_r,$$

and  $H(\vec{x}, \vec{x}')$  is the coalescence kernel. Like in the one dimensional case the kernel will be here independent on time and we will consider, in the numerical simulations, only the constant case:  $H(\vec{x}, \vec{x}') = 1$ .

Let us define the multidimensional moment of order  $p$ ,  $\mathcal{M}_p(t)$ , by:

$$\mathcal{M}_p(t) = \int_0^{\infty} \prod_{r=1}^d x_r^{\alpha_r} f(\vec{x}, t) d\vec{x} \quad (3.2)$$

where the powers  $\alpha_r$  are such that:

$$\sum_{r=1}^d \alpha_r = p.$$

It is easily seen that, choosing  $\alpha_r = 0$  for each  $r$ , we obtain the zero order moment:

$$\mathcal{M}_0(t) = \int_0^{\infty} f(\vec{x}, t) d\vec{x},$$

which represents the density number of particles and is decreasing in time.

Concerning the first order moment, we may choose one particular dimension  $\hat{r}$  for which the power  $\alpha_{\hat{r}}$  is equal to 1, and fix all the other powers to zero:

$$\alpha_r = \begin{cases} 1 & r = \hat{r} \\ 0 & \text{otherwise.} \end{cases}$$

Then the first order moment given by:

$$\mathcal{M}_1(t) = \int_0^\infty x_{\hat{r}} f(\vec{x}, t) d\vec{x},$$

represents the total size in the  $\hat{r}$  dimension and is constant in time. Moreover, from the conservation of each first order moment for  $r = 1, \dots, d$ , we can easily obtain the conservation of

$$\int_0^\infty \Phi(\vec{x}) f(\vec{x}, t) d\vec{x},$$

for all linear combination  $\Phi(\vec{x})$  of  $x_r$ , and in particular for the sum over all  $x_r$ :  $\Phi(\vec{x}) = \sum_{r=1}^d x_r$ . We will see that while at a continuous level all (with respect to each dimension  $r$ ) first order moments are conserved, this will not be the case at the discrete level.

We finally recall that in the multidimensional framework too, the moments of order larger than  $p = 1$  are increasing in time.

We now detail the numerical scheme. Applying the same arguments as in the one-dimensional case, we can consider the finite volume scheme approximating (3.1) and involving the overlap of created cells with the existing mesh. Whereas, concerning the conservation of the discrete first moment, it is possible to conserve only one of the first order moments.

Let us split  $\mathbb{R}_+^d$  in the cells  $I_r = [x_{I_r-1/2}, x_{I_r+1/2}]$ , for each dimension  $r = 1, \dots, d$  and with as usual  $x_{-1/2} = 0$ . Moreover, let us define the grid points, for each  $r = 1 \dots d$ , by:

$$x_{I_r} = \frac{x_{I_r-1/2} + x_{I_r+1/2}}{2},$$

and the mesh step along each dimension by:

$$\Delta x_{I_r} = x_{I_r+1/2} - x_{I_r-1/2},$$

so that the whole mesh step is given by:

$$\Delta \vec{x}_I = \prod_{r=1}^d \Delta x_{I_r}.$$

Moreover, let us define the discrete distribution function on the cell  $I$  at the iteration  $n$  by  $f_I^n = f(x_{I_1}, \dots, x_{I_d}, t^n)$ . Then the numerical scheme reads:

$$f_I^{n+1} = f_I^n + \Delta t^n \left( \frac{1}{2} \sum_{(K,J) \in S^I} \tilde{H}_{J,K} f_K f_J \lambda_{J,K}^I \frac{\Delta \vec{x}_J \Delta \vec{x}_K}{\Delta \vec{x}_I} - \sum_{J=0}^\infty H_{I,J} f_I f_J \Delta \vec{x}_J \right) \quad (3.3)$$

where the  $\sum_{(J,K) \in S^I}$  is now the product of all the sums for  $r = 1, \dots, d$ :

$$\sum_{(J,K) \in S^I} = \prod_{r=1}^d \sum_{(J_r, K_r) \in S^{I_r}}$$

and the set  $S^{I_r}$  are defined analogously as in the one dimensional case:

$$S^{I_r} = \{(J_r, K_r) \in \mathbb{N} \times \mathbb{N} : (J_r + K_r) \cap I_r \neq \emptyset\},$$

and represent, for each dimension  $r$ , the sum over all cells  $K_r$  such that the intersection between the cell  $J_r + K_r$  and  $I_r$  is not empty.

Moreover, in (3.3),  $\lambda_{J,K}^I$  is the proportionality factor and is generalized as follows. Let us define, for  $r = 1, \dots, d$  the following minimum and maximum:

$$\overline{m_{J_r, K_r}^{I_r}} = \max(\vec{x}_{I_r-1/2}, \vec{x}_{J_r-1/2} + \vec{x}_{K_r-1/2})$$

$$\underline{m_{J_r, K_r}^{I_r}} = \min(\vec{x}_{I_r+1/2}, \vec{x}_{J_r+1/2} + \vec{x}_{K_r+1/2}),$$

then the multi-dimensional parameter  $\lambda_{J,K}^I$  is given by:

$$\lambda_{J,K}^I = \prod_{r=1}^d \left( \frac{\overline{m_{J_r, K_r}^{I_r}} - \underline{m_{J_r, K_r}^{I_r}}}{\Delta \vec{x}_{J_r} + \Delta \vec{x}_{K_r}} \right)_+. \quad (3.4)$$

As announced, all the first order moments are conserved at a continuous level, so that we have several possibilities for defining the modified kernel  $\tilde{H}_{J,K}$ , but we cannot conserve at the discrete level all the first order moments, see also [17] in which for the two dimensional case, the authors conserve the first moment associated to the linear combination  $\Phi(x, y) = x + y$ . Generalizing the proof of section 2.2, the modified kernel  $\tilde{H}_{J,K}$  preserving the first moment associated to a general linear combination  $\Phi(\vec{x})$ , is given by:

$$\tilde{H}_{J,K} = H_{J,K} \frac{(\Phi_J + \Phi_K)}{\sum_{I \in R_{J,K}} \Phi_I \lambda_{J,K}^I}, \quad (3.5)$$

where the sets  $R_{J,K}$  are defined by:

$$R_{J,K} = \prod_{r=1}^d R_{J_r, K_r}$$

with:

$$R_{J_r, K_r} = \{I_r \in \mathbb{N} : I_r \cap J_r + K_r \neq \emptyset\}.$$

**4. Numerical results.** In order to validate our scheme, we perform some of the numerical tests done in [7] and [12] for the one dimensional problem and the gelation phenomena, and those in [17], for the two dimensional case.

Before detailing the tests, we recall that the sum in the loss term is defined up to infinity, see (2.4), and when performing numerical computing we must to truncate it, see also [7]. The choice of the truncation value  $x_{max}$ , corresponding to the maximum value for the  $x$  dimension, has to be evaluated accurately, as it will be shown in the sequel.

We choose to apply our numerical scheme with the following uniform (1, 2, 3 and 4) and nonuniform (5, 6 and 7) meshes:

1.  $\Delta x = 0.1$ ,  $x_{max} = 50$

2.  $\Delta x = 0.5, x_{max} = 50$
3.  $\Delta x = 0.01, x_{max} = 50$
4.  $\Delta x = 0.5, x_{max} = 2500$
5.  $x_i = x_{max} 2^{(i-N)/3}, x_{max} = 5000, N = 150$  points
6.  $x_i = x_{max} 2^{(i-N)/3}, x_{max} = 500000, N = 165$  points
7.  $x_i = x_{max} 2^{(i-N)/6}, x_{max} = 5000, N = 300$  points

Since we want to save about a thousand values in time for our numerical solutions, at each time iteration we choose the time step as the minimum between the one defined by the CFL condition (2.18) and  $10^{-3}$ . Finally, we stop computations either when time is equal to  $t = 1.5$  or when 2% of the mass is lost.

**4.1. One dimensional case:**  $H(x, x') = 1$ . We now consider the one dimensional case with the constant kernel  $H(x, x') = 1$  and compare our results with those in [7]. We define the following initial condition:

$$f_0(x) = e^{-x}.$$

We recall that in this case, see [7] and references therein, the coalescence equation admits the following analytic solution:

$$f(x, t) = \left( \frac{2}{2+t} \right)^2 \exp\left( \frac{-2x}{2+t} \right), \quad (4.1)$$

with the zero and first moments respectively given by:

$$\mathcal{M}_0(t) = \frac{2}{2+t}, \quad \mathcal{M}_1(t) = 1.$$

In figure 4.1 we trace the zero (left) and first (right) order moments against the analytical solution (blue line). While for the zero order moment we can barely see the difference between the various mesh choices, concerning the first order moment, we note that each mesh choice is constant in time, but the starting value is not the good one when applying nonuniform meshes. This error is due to the quadrature formula we apply to compute the initial first order moment. Moreover, the better fit seems to be given by test number 3, that is the uniform mesh with the smallest space step. Nevertheless, we must recall that nonuniform meshes allow us to compute solutions on bigger domains, i.e. for larger values of  $x_{max}$ , than uniform ones, with still an acceptable error.

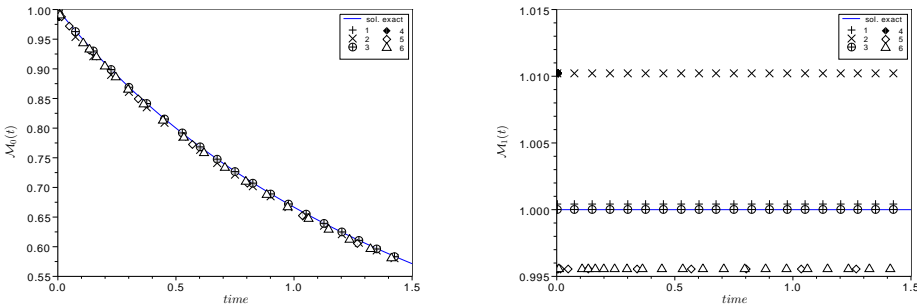


FIG. 4.1.  $H(x, x') = 1$ : zero (left) and first (right) order moments.

We also consider, as done in [7], the discrete  $L_1$  error defined by:

$$\epsilon = \sum_{i=0}^N \Delta x_i |f(x_i, t_n) - f_i^n|, \quad (4.2)$$

and we compute it for the uniform mesh with  $N = 125, 250, 500$  and truncation  $x_{max}=50$ . The result is shown in figure 4.2 both in normal (left) and logarithmic (right) scale. We can see that our scheme is second order accurate, as we may expect since all integrals in our discretization are approximated by the midpoint quadrature formula.

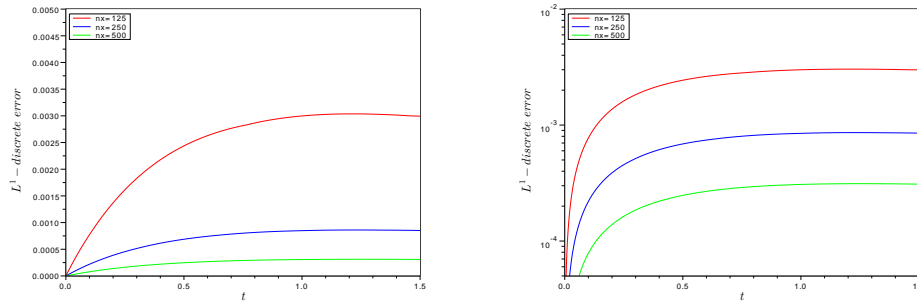


FIG. 4.2.  $H(x, x') = 1$ :  $\epsilon$  in normal (left) and logarithmic (right) scale.

**4.2. One dimensional case:**  $H(x, x') = x + x'$ . We now consider one of the one dimensional tests performed in [17]. We define the initial condition

$$f_0(x) = e^{-x},$$

then the analytical solution reads:

$$f(x, t) = \frac{1 - \alpha}{x\sqrt{\alpha}} I_1(2x\sqrt{\alpha}) e^{-x(1+\alpha)}, \quad \text{with } \alpha = 1 - e^{-t}$$

and the moments of order zero, one and two are given by:

$$\mathcal{M}_0(t) = e^{-t}, \quad \mathcal{M}_1(t) = 1, \quad \mathcal{M}_2(t) = e^{2t}$$

We compute the numerical solution applying the nonuniform mesh of test 5, but with  $N = 40$  and  $x_{max} = 2000$ , as done in [17]. We stop the computation once the first order moment begin to decrease, because of the truncation value. The results are shown in figure 4.3 where we have traced, in logarithmic scale, the analytical moments up to the second order and the numerical one up to the third order. We can see that our third order moment is always increasing, while the one given in [17] is not monotone.

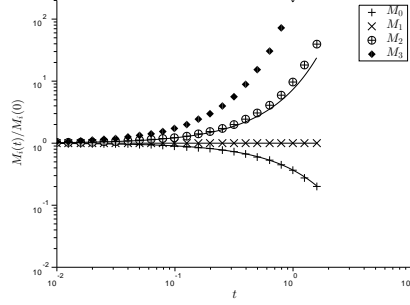


FIG. 4.3.  $H(x, x') = x + x'$ : zero, first, second and third order moments.

**4.3. One dimensional case:**  $H(x, x') = xx'$ . We consider now the one dimensional case with multiplicative kernel  $H(x, x') = xx'$  which is well known to yield to gelation. Following [7], we choose the following initial condition:

$$f_0(x) = \frac{e^{-x}}{x}$$

for which the coalescence problem admits the analytical solution:

$$f(x, t) = e^{-Tx} \frac{I_1(2x\sqrt{t})}{x^2\sqrt{t}}, \quad (4.3)$$

with the value  $T$  defined by:

$$T = \begin{cases} 1 + t & \text{if } t \leq 1 \\ 2\sqrt{t} & \text{otherwise} \end{cases} \quad (4.4)$$

and  $I_1$  the modified Bessel function at order one:

$$I_1(z) = \frac{1}{\pi} \int_0^\pi \exp(z \cos(\theta)) \cos(\theta) d\theta. \quad (4.5)$$

Again the first order moment can be computed and is given by:

$$\mathcal{M}_1(t) = \begin{cases} 1 & \text{if } t < 1 \\ t^{-1/2} & \text{otherwise} \end{cases}$$

We note that when  $t = 1$  the gelation phenomena takes place: the first order moment is no more conserved.

In figure 4.4, we compare the normalized first order moment obtained by our numerical simulation applying the uniform meshes 1, 2 and 3 (left) or the nonuniform meshes 5 and 7 (right) to the analytical solution truncated respectively at  $x_{max} = 50$  (red line) or  $x_{max} = 5000$  (cyan line). We also trace the exact analytical solution (blue line). The results given by 1, 2 and 3 fit well the red line, but we observe a little overestimation once the gelation phenomena takes place. This may be due to the very small truncation value we choose. Concerning the nonuniform meshes, we

note that, as expected, the finest mesh given by test 7 has a better fit with the cyan line. Finally, we remark that nonuniform meshes allow us to compute solutions with a larger truncation value  $x_{max}$ .

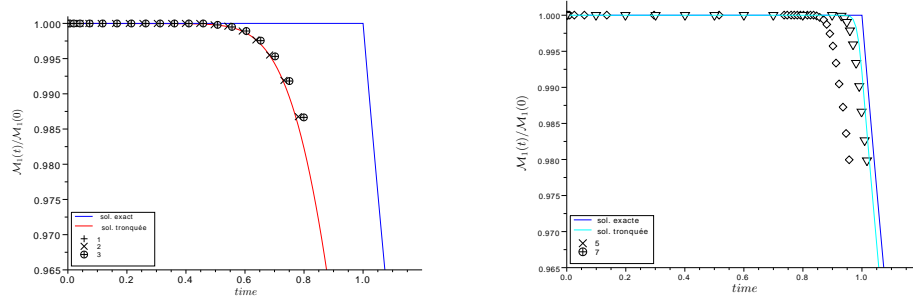


FIG. 4.4.  $H(x, x') = xx'$ : uniform meshes 1, 2, 3 (left) and nonuniform meshes 5 and 7 (right).

Moreover, as done for the constant kernel and as done in [7], we compute the discrete  $L_1$  error defined by (4.2) for the uniform mesh with  $N = 125, 250, 500$  and truncation  $x_{max}=50$ . The result is shown in figure 4.5 both in normal (left) and logarithmic (right) scale. As expected the scheme is second order accurate.

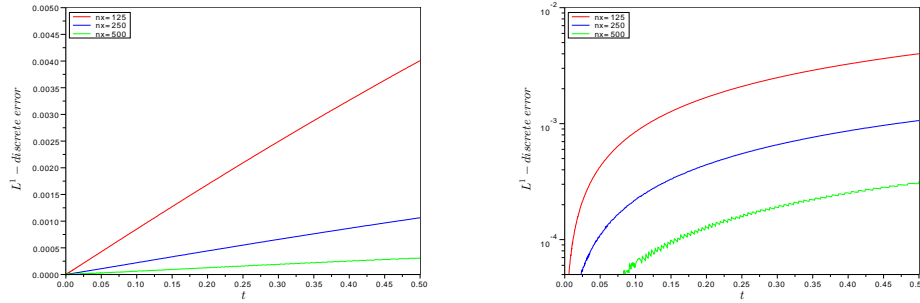


FIG. 4.5.  $H(x, x') = 1: \epsilon$  in normal (left) and logarithmic (right) scale.

We finally remark that when computing moments of order bigger than 1, we obtain the same behavior as in [7], that is, as time approach the gelation time, the moments of order  $p \geq 3/2$  blow up.

**4.4. Two dimensional validation.** In this section, we compare our numerical results with those obtained in [17]. Before entering the details, let us write the general formula for a moment of order  $p = r + s$ , in two dimensions:

$$\mathcal{M}_{r,s}(t) = \int_0^\infty \int_0^\infty x^r y^s f(t, x, y) dx dy.$$

Following [17], we assume a constant coalescence kernel  $H(\vec{x}, \vec{x}') = 1$  and we compute the solution up to a final time  $t = 100$ . We consider the following initial

condition:

$$f_0(x, y) = e^{-x-y}.$$

The analytical solution reads, see also [16] :

$$f(t, x, y) = \frac{4 e^{-x-y}}{(t+2)^2} I_0(\theta), \quad \text{with} \quad \theta = \sqrt{\frac{4t}{t+2}}$$

and  $I_0$  the modified Bessel function of first kind of order zero. The zero and first order moments associated with this solution are given by, see [17]:

$$\mathcal{M}_{0,0}(t) = \frac{2}{2+t}, \quad \mathcal{M}_{1,0}(t) = \mathcal{M}_{0,1}(t) = 1, \quad \mathcal{M}_{1,1}(t) = 1+t.$$

In figure 4.6 we plot in logarithmic scale the analytical solution at time  $t = 100$  defined for the nonuniform mesh 5 where we have fixed the number of discretization points to  $N = N_x = N_y = 40$ , and choose a truncation value  $x_{max} = y_{max} = 1000$ .

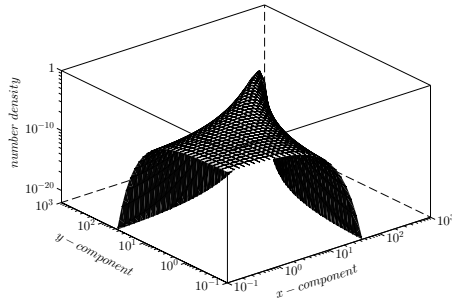


FIG. 4.6.  $f_0(x, y) = e^{-x-y}$ : analytical solution at  $t = 100$

We now remark, figure 4.7 (right), that all our numerical moments fit well all the analytical one (red lines). Moreover, concerning our the numerical solution  $f(t, x, y)$ , figure 4.7 (left), is smooth, but has a little diffused with respect to the analytical one. We recall that the numerical results in [17], has a good fit for the moments too, whereas the numerical solution  $f(t, x, y)$  has singularities, but has less diffused.

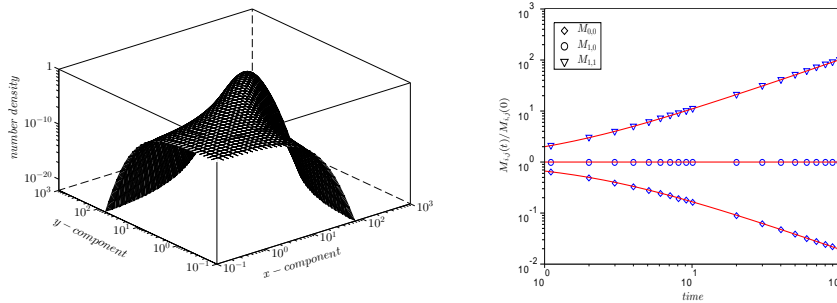


FIG. 4.7.  $f_0(x, y) = e^{-x-y}$ : Computed solution (left). Zero first and second order moments (right).

We now consider a final test also performed in [17]. As for the previous test, we choose the nonuniform mesh given by 5, with  $N = N_x = N_y = 40$  and  $x_{max} = y_{max} = 1000$ , the constant coalescence kernel  $H(\vec{x}, \vec{x}') = 1$  and the final computational time  $t = 100$ . But now the initial condition is defined by:

$$f_0(x, y) = 16xy e^{-2(x+y)}.$$

In this case the analytical solution is given by, see [9]:

$$f(t, x, y) = \frac{8}{\sqrt{t(t+2)}^3} e^{-2(x+y)} [\text{I}_0(\theta) - \text{J}_0(\theta)],$$

where

$$\theta = 4\sqrt{xy} \left( \frac{t}{t+2} \right)^{1/4}$$

Here  $\text{J}_0$  and  $\text{I}_0$  are respectively, the Bessel function and the modified Bessel function of first kind of order zero. For this solution [17] gives as [20], the analytical solution for the following moments :

$$\mathcal{M}_{0,0}(t) = \frac{2}{2+t},$$

$$\mathcal{M}_{1,0}(t) = \mathcal{M}_{0,1}(t) = 1,$$

$$\mathcal{M}_{2,0}(t) = \frac{3+2t}{2}, \quad \mathcal{M}_{1,1}(t) = 1+t,$$

$$\mathcal{M}_{3,0}(t) = \frac{3(1+t)(2+t)}{2}, \quad \mathcal{M}_{2,1}(t) = \frac{(3+7t+3t^2)}{2}.$$

The exact solution at  $t = 100$  is traced in figure 4.8, where again the graph is in logarithmic scale:

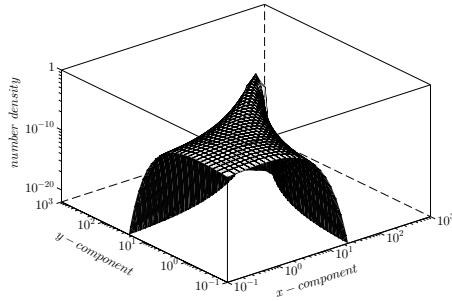


FIG. 4.8.  $f_0(x, y) = 16xy e^{-2(x+y)}$ : analytical solution at  $t = 100$

In figure 4.9 we trace the numerical moments we compute and the analytical one given by the previous formula (right). We note a better agreement than those

obtained in [17], in particular for the higher order moments. Moreover, concerning our numerical solution (left), we still have slightly diffused, but we have a smooth solution, whereas in [17] the numerical solution still have singularities, but seems to have not diffused.

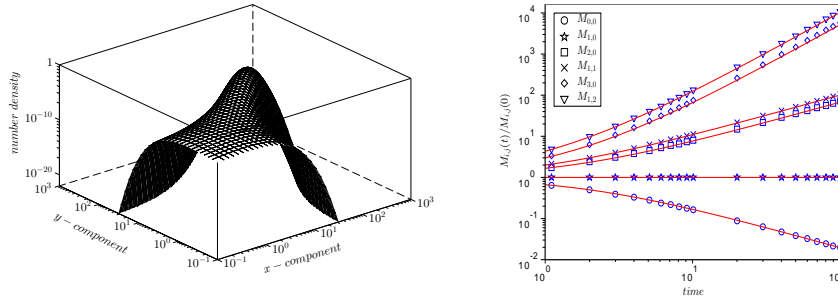


FIG. 4.9.  $f_0(x, y) = 16xy e^{-2(x+y)}$ : Computed solution (left). Computed moments (right).

**5. Conclusion.** In this paper we have described a finite volume discretization of the coalescence equation (1.1) which conserves the first order moment. Moreover, this numerical scheme is suitable both for uniform and nonuniform meshes, and deal with the overlaps of created cells proportionally distributing it over the defined meshes. The scheme is second order accurate and consistent with the continuous formulation of the coalescence problem. Finally, the generalization to a multidimensional framework has been detailed, too.

The code has been validate considering the following classical tests:  $H(x, x') = 1, x + x', xx'$ , for which analytical solutions to (1.1) as well as their moments have been recalled. We also have compared our numerical results with those already existing in the literature, in particular with those published in [7] and [17]. Our numerical scheme shows a good agreement with all the considered tests, and seems to behave better than the one in [17], at least concerning the smoothness of the analytical solution and the computation of higher order moments. Still some work may be done in order to reduce the observed numerical diffusion, for example, refining the way the created cells are distributed over the existing mesh.

#### REFERENCES

- [1] H. Babovsky, *On a Monte Carlo scheme for Smoluchowski's coagulation equation*, Monte Carlo Methods Appl., 5,1–18, (1999).
- [2] A. Burgisser and J.E. Gardner, *Experimental constraints on degassing and permeability in volcanic conduit flow*, Bull. Volcanol. **67** (2005) 42–56
- [3] M. Deaconu, N. Fournier, E. Tanré, *Study of a stochastic particle system associated with the Smoluchowski coagulation equation*, Methodol. Comput. Appl. Probab., 5, 131–158, (2003).
- [4] L. D. Erasmus, D. Eyre, R. C. Everson, *Numerical treatment of the population balance equation using a Spline-Galerkin method*, Computers Chem. Engrg., 8, 775–783, (1994).
- [5] A. Eibeck, W. Wagner, *An efficient stochastic algorithm for studying coagulation dynamics and gelation phenomena*, SIAM J. Sci. Comput., 22, 802–821, (2000).
- [6] A. Eibeck, W. Wagner, *Stochastic particle approximations for Smoluchowski's coagulation equation*, Ann. Appl. Probab., 11, 1137–1165, (2001).
- [7] F. Filbet, P. Laureçot, *Numerical simulation of the Smoluchowski equation*, SIAM J. Sci. Comput., **25**, 2004–2028, (2004).

- [8] L. Forestier-Coste, S. Mancini, A. Burgisser, F. James, *A monodisperse model for bubbles growth in magmas*, (submitted).
- [9] F. Gelbard, J.H. Seinfeld, *Coagulation and growth of a multicomponent aerosol*. Journal of Colloid and Interface Science **63** (3), 357–375, (1978).
- [10] D. S. Krivitsky, *Numerical solution of the Smoluchowski kinetic equation and asymptotics of the distribution function*, J. Phys. A, 28, 2025–2039, (1995).
- [11] R. Kumar, J. Kumar, G. Warneke, *Numerical methods for solving two-dimensional aggregation population balance equations*, Chemical Engineering Science, **35**, 6, 999–1009, (2011).
- [12] J. Kumar, M. Peglow, G. Warneke, S. Heinrich, *An efficient numerical technique for solving population balance equation involving aggregation, breakage, growth and nucleation*, Powder Technology, **182**, 81–104, (2008).
- [13] M. H. Lee, *On the validity of the coagulation equation and the nature of runaway growth*, Icarus, 143, 74–86, (2000).
- [14] M. H. Lee, *A survey of numerical solutions to the coagulation equation*, J. Phys. A, 34, 10219–10241, (2001).
- [15] F. Leyvraz, H. R. Tschudi, *Singularities in the kinetics of coagulation processes*, J. Phys. A, 14, pp. 3389–3405, (1981).
- [16] A.A. Lushnikov, *Evolution of coagulating systems III. Coagulating mixtures*. Journal of Colloid and Interface Science **54** (1), 94–101, (1976).
- [17] S. Qamar, G. Warnake, *Solving population balance equations for two-component aggregation by a finite-volume scheme*, Chemical Engineering Science, **62**, 679–693, (2007).
- [18] M. Smoluchowski, *Drei Vorträge über Diffusion, Brownsche Molekularbewegung und Koagulation von Kolloidteilchen*, Physik. Zeitschr., 17, 557–599, (1916).
- [19] H. Tanaka, S. Inaba, K. Nakaza, *Steady-state size distribution for the self-similar collision cascade*, Icarus, 123, 450–455, (1996).
- [20] H.M. Vale, T.F. Mckenna, *Solution of the population balance equation for two-component aggregation by an extended fixed pivot technique*, Industrial & Engineering Chemistry Research **44** (20), 7885–7891, (2005).
- [21] A. Wiles, *Modular elliptic curves and Fermat's last theorem*, Ann. Math., 141, 443–551, (1995).